PAPER

Non-orthogonal Access Scheme over Multiple Channels with Iterative Interference Cancellation and Fractional Sampling in OFDM Receiver

Hiroyuki OSADA[†a)], **Mamiko INAMORI**[†b)], ***Student Members***, ***and*** **Yukitoshi SANADA**[†c)], ***Member***

SUMMARY A diversity scheme with Fractional Sampling (FS) in OFDM receivers has been investigated recently. FS path diversity makes use of the imaging components of the desired signal transmitted on the adjacent channel. To increase the diversity gain with FS the bandwidth of the transmit signal has to be enlarged. This leads to the reduction of spectrum efficiency. In this paper non-orthogonal access over multiple channels in the frequency domain with iterative interference cancellation (IIC) and FS is proposed. The proposed scheme transmits the imaging component non-orthogonally on the adjacent channel. In order to accommodate the imaging component, it is underlaid on the other desired signal. Through diversity with FS and IIC, non-orthogonal access on multiple channels is realized. Our proposed scheme can obtain diversity gains for non-orthogonal signals modulated with QPSK.

key words: *fractional sampling, OFDM, path diversity, interference cancellation*

1. Introduction

Orthogonal frequency division multiplexing (OFDM) has been used as a modulation scheme in various wireless communication systems such as terrestrial digital broadcasting, wireless broadband communications, or wireless local area networks. This is because an OFDM scheme employs long symbol duration and the relative amount of multipath delay spread reduces [1], [2].

Meanwhile, diversity is necessary to improve the performance of the OFDM system on the multipath channel. One of the typical diversity techniques is antenna diversity [3]. Multiple antenna elements must be spatially separated in order to reduce the correlation among the received signals [4], [5]. However, it is difficult for small terminals to implement multiple antenna elements. Therefore, a FS scheme that realizes diversity with a single antenna has also been proposed [6]. The FS scheme achieves path diversity by sampling a received signal at a rate higher than the symbol rate and by demodulating the received samples over multiple demodulation branches in parallel.

FS path diversity makes use of the imaging components of the desired signal transmitted on the adjacent channel. A non-orthogonal access scheme with the use of FS and decision feedback cancellation has been evaluated [7]. In [7], non-orthogonal access in which the part of the signal for one user overlaps with that of another user in the frequency domain is assumed. Both of the users can demodulate the signals if their transmission powers have a large difference. This implies that non-orthogonal access can be implemented only when the distances of users from the base station are different. In this situation, the signal with larger power can be cancelled only with a single cancellation process. If the distances from the base station are almost the same, the interference cannot be removed due to the decision errors in the first demodulation.

On the other hand, in this paper, to equalize the quality of the communication links, the signals for both of the users include the imaging components and they are underlaid to the desired signals each other. The powers of the imaging components are set to be smaller to improve the performance of the first demodulation. Furthermore, with the use of FS, an iterative interference cancellation (IIC) scheme is introduced to reduce the residual interference. It is demonstrated that the proposed scheme can obtain diversity gains for non-orthogonal signals modulated with QPSK and transmitted with the same total transmission power.

This paper is organized as follows. In Sect. 2, the system model with the proposed cancellation scheme is described. Section 3 shows numerical results obtained through computer simulation. The conclusions of this paper are presented in Sect. 4.

2. Channel Allocation and Cancellation Process

Figure 1 shows the channel allocation model of the proposed scheme. It is for the downlinks of two different terminals.

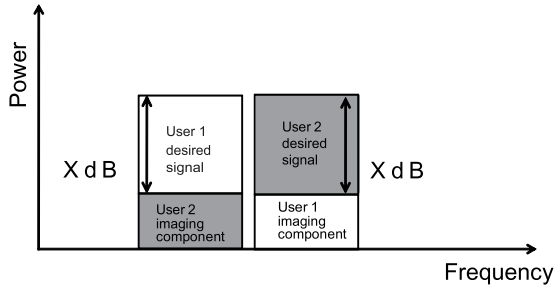

Fig. 1 Channel allocation model.

Manuscript received March 12, 2012.
Manuscript revised August 4, 2012.

[†]The authors are with the Dept. of Electronics and Electrical Engineering, Keio University, Yokohama-shi, 223-8522 Japan.
a) E-mail: hosada@snd.elec.keio.ac.jp
b) E-mail: inamori@snd.elec.keio.ac.jp
c) E-mail: sanada@elec.keio.ac.jp

DOI: 10.1587/transcom.E95.B.3837

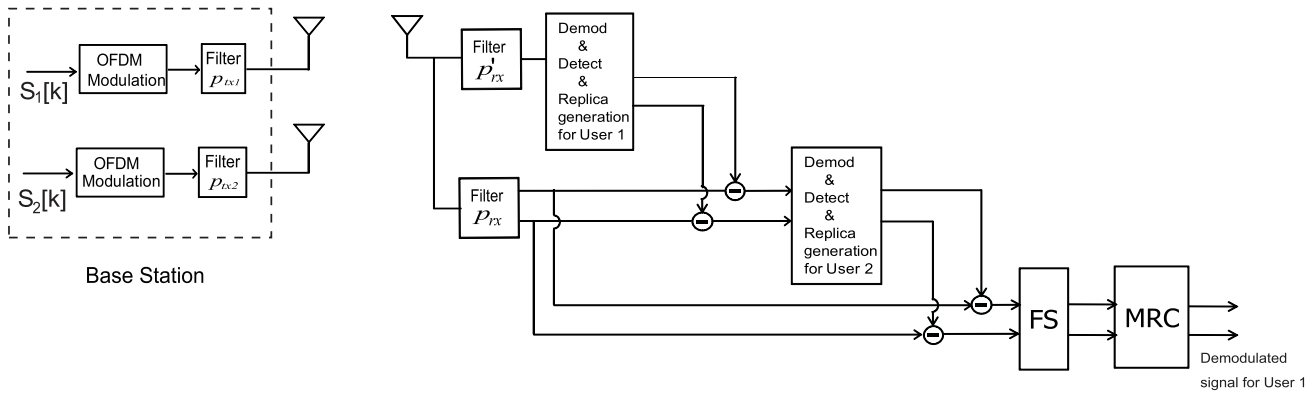

Fig. 2 Block diagram of system model.

The OFDM signals for User 1 and 2 are transmitted on the adjacent two channels. The symbol timings of those signals are synchronized to avoid the inter-carrier interference between the users. Their imaging components are underlaid non-orthogonally on the other desired signals, respectively. The powers of the imaging components are X dB smaller than the desired signals on both of the channels. Therefore, the non-orthogonal overlaid or underlaid signal has to be cancelled in order to demodulate the desired signal. A block diagram of the proposed FS-OFDM receiver is shown in Fig. 2. At the receiver, the desired signal components of User 1 ($S_1[k]$) and User 2 ($S_2[k]$) pass through the analog filters whose impulse responses are given as $p'_{rx}(t)$ and $p_{rx}(t)$. First, the User 1 signal through $p'_{rx}(t)$ is demodulated, its replica is regenerated, and the replica signal is subtracted from the received signal through $p_{rx}(t)$. After the subtraction, the User 2 signal is demodulated with FS, and it's replica is regenerated, and the replica signal is subtracted from the received signal through $p_{rx}(t)$. The cancellation of the signal from User 2 is then realized.

The OFDM signals of User 1 and User 2 are given as

$$u_1[n] = \frac{1}{\sqrt{N}} \sum_{k=-N/2}^{N/2-1} S_1[k] \exp\left(j\frac{2\pi nk}{N}\right), \quad (1)$$

$$u_2[n] = \frac{1}{\sqrt{N}} \sum_{k=-N/2}^{N/2-1} S_2[k] \exp\left(j\frac{2\pi nk}{N}\right), \quad (2)$$

where $S_1[k]$ and $S_2[k]$ are the information symbols on the kth subcarrier for User 1 and User 2, respectively, $n(n = 0, 1, ..., 2N-1)$ is the time index, and N is the size of the inverse discrete Fourier transform (IDFT). Then, $u_1[n]$ and $u_2[n]$ pass through different transmit filters. These signals can be generated by IDFT with the size of $2N$ in the base station at a time. However, they are treated separately in this paper for the convenience of representation. Suppose the last part of the OFDM signal is replicated and appended at the beginning as a guard interval (GI), the transmit signals in the baseband form are given by

$$x_1(t) = \sum_{n=-N_{GI}}^{N-1} u_1[n] p_{tx1}(t - nT_s), \quad (3)$$

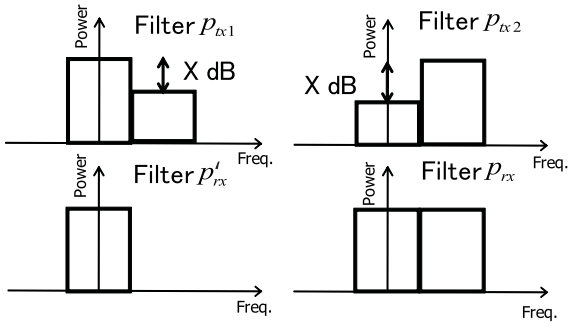

Fig. 3 Frequency response of filters.

$$x_2(t) = \sum_{n=-N_{GI}}^{N-1} u_2[n] p_{tx2}(t - nT_s), \quad (4)$$

where $p_{tx1}(t)$ and $p_{tx2}(t)$ are the impulse responses of the respective transmit filters that include the responses of bandpass filters at D/A converters, T_s is the sampling interval for the OFDM signal, and N_{GI} is the GI length. The transmit filters for the User 1 and User 2 signals have the symmetric frequency responses as shown in Fig. 3. At the receiver two different baseband filters are used as shown in Fig. 3. The filter $p'_{rx}(t)$ has the passband only on the channel for the desired signal component of User 1. Figure 4 shows the proposed cancellation scheme. The signal that passes through $p'_{rx}(t)$ is used for the tentative decision of the User 1 signal. The replica signal is regenerated, subtracted from the received signal that passes through the filter $p_{rx}(t)$. The signal for User 2 is then demodulated with FS, it's replica is regenerated, and subtracted from the signal output from the filter $p_{rx}(t)$.

2.1 First Cancellation

The received signal through $p'_{rx}(t)$ is given as

$$y'(t) = y'_1(t) + y'_2(t) + v'(t) \quad (5)$$

where $y'_1(t)$ and $y'_2(t)$ represent the signals of User 1 and User 2 that are

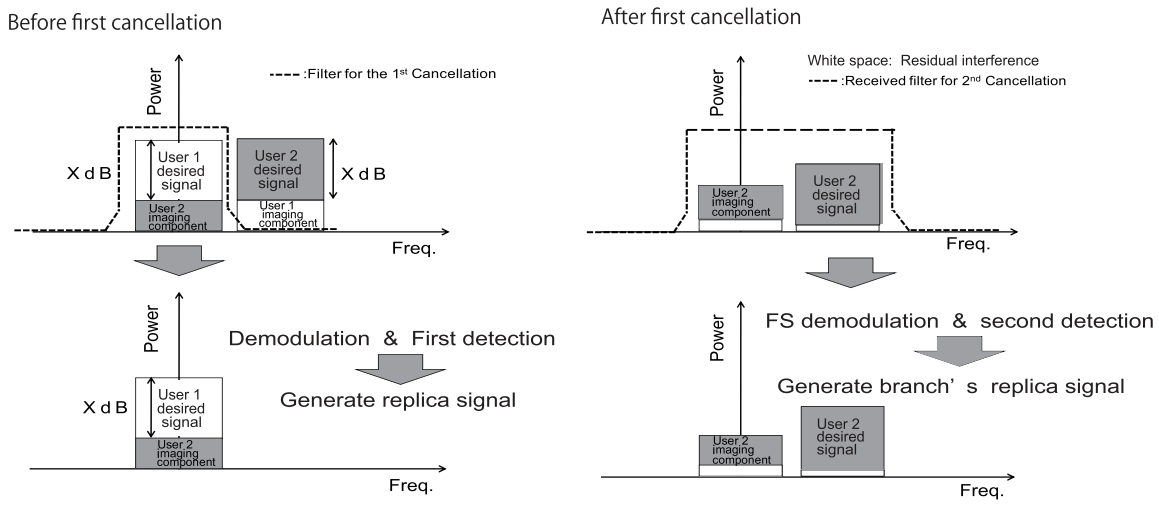

Fig. 4 Proposed cancellation scheme.

$$y'_1(t) = \sum_{n=-N_{GI}}^{N-1} u_1[n]h'_1(t-nT_s), \tag{6}$$

$$y'_2(t) = \sum_{n=-N_{GI}}^{N-1} u_2[n]h'_2(t-nT_s), \tag{7}$$

and $v'(t)$ is the noise through the filter $p'_{rx}(t)$. On the other hand, the received signal through the filter $p_{rx}(t)$ is given as

$$y(t) = y_1(t) + y_2(t) + v(t) \tag{8}$$

where $y_1(t)$ and $y_2(t)$ represent the signals of User 1 and User 2 that are

$$y_1(t) = \sum_{n=-N_{GI}}^{N-1} u_1[n]h_1(t-nT_s), \tag{9}$$

$$y_2(t) = \sum_{n=-N_{GI}}^{N-1} u_2[n]h_2(t-nT_s), \tag{10}$$

and $v(t)$ is the noise through $p_{rx}(t)$. Since these signals are transmitted through multipath channels with the independent impulse responses of $c_1(t)$ and $c_2(t)$ for User 1 and User 2, $h'_1(t)$, $h'_2(t)$, $h_1(t)$ and $h_2(t)$ are the impulse responses of the composite channels that are given as

$$h'_1(t) = p_{tx1}(t) \star c_1(t) \star p'_{rx}(t), \tag{11}$$

$$h'_2(t) = p_{tx2}(t) \star c_2(t) \star p'_{rx}(t), \tag{12}$$

$$h_1(t) = p_{tx1}(t) \star c_1(t) \star p_{rx}(t), \tag{13}$$

$$h_2(t) = p_{tx2}(t) \star c_2(t) \star p_{rx}(t), \tag{14}$$

where $\star$ denotes convolution. The signal after $p_{rx}(t)$ is converted to digital samples by the A/D converter at the rate of T_s for the first cancellation. Therefore, the received digital signal is expressed as

$$y'[n] = y'(nT_s) \tag{15}$$

where T_s is the sampling rate. After removing the GI and taking the DFT to N samples, the signal on the kth subcarrier is

$$\begin{aligned} Z'[k] &= \sum_{n=0}^{N-1} y'[n] \exp\left(-\frac{j2\pi nk}{N}\right) \\ &= H'_1[k]S_1[k] + H'_2[k]S_2[k] + W'[k] \end{aligned} \tag{16}$$

where $H'_1[k]$ and $H'_2[k]$ are the frequency responses of the User 1 and 2 signals and $W'[k]$ is the noise through $p'_{rx}(t)$ on the kth subcarrier. These are calculated as

$$H'_1[k] = \sum_{n=0}^{N-1} h'_1[n] \exp\left(-\frac{j2\pi nk}{N}\right), \tag{17}$$

$$H'_2[k] = \sum_{n=0}^{N-1} h'_2[n] \exp\left(-\frac{j2\pi nk}{N}\right), \tag{18}$$

$$W'[k] = \sum_{n=0}^{N-1} v'[n] \exp\left(-\frac{j2\pi nk}{N}\right), \tag{19}$$

where $h'_1[n]$, $h'_2[n]$, and $v'[n]$ are given by

$$h'_1[n] = h'_1(nT_s), \tag{20}$$

$$h'_2[n] = h'_2(nT_s), \tag{21}$$

$$v'[n] = v'(nT_s). \tag{22}$$

Suppose that the estimated frequency response on the kth subcarrier of the User 1 signal is expressed as $\hat{H}'_1[k]$, the demodulated signal on the adjacent channel is

$$\tilde{S'}_1[k] = \frac{\hat{H}'^*_1[k]Z'[k]}{\hat{H}'^*_1[k]\hat{H}'_1[k]}. \tag{23}$$

The symbol of the User 1 signal, $\hat{S'}_1[k]$, is detected with $\tilde{S'}_1[k]$. Therefore, the replica of the User 1 signal on all the branches of FS is given in the $G \times 1$ vector form as

$$\hat{\mathbf{Y}}_1[k] = \mathbf{H}_1[k]\hat{S'}_1[k]. \tag{24}$$

In the meantime, the signal after $p_{rx}(t)$ is converted to digital samples by the A/D converter at the rate of T_s/G with FS.

$$y_g[n,g]=\sum_{l=0}^{P-1} u_1[l]h_1[n-l,g]+\sum_{l=0}^{P-1} u_2[l]h_2[n-l,g]+v[n,g],$$
$$g=0,...,G-1, \tag{25}$$

where $y_g[n]$, $h_{1,g}[n]$, $h_{2,g}[n]$ and $v_g[n]$ are the polynomials of sampled $y(t)$, $h_1(t)$, $h_2(t)$ and $v(t)$, respectively, and are given as

$$y_g[n,g] := y(nT_s + gT_s/G), \tag{26}$$
$$h_1[n,g] := h_1(nT_s + gT_s/G), \tag{27}$$
$$h_2[n,g] := h_2(nT_s + gT_s/G), \tag{28}$$
$$v[n,g] := v(nT_s + gT_s/G). \tag{29}$$

These samples are put into G DFT demodulators in parallel and the sampling rate on each branch reduces to $1/T_s$. Therefore, the images are fold down to the main channel as alias components. After removing the GI and taking DFT on each subcarrier, the received symbol is given by

$$\mathbf{Z}[k] = \mathbf{H}_1[k]S_1[k] + \mathbf{H}_2[k]S_2[k] + \mathbf{W}[k] \tag{30}$$

where $\mathbf{Z}[k] = [Z[k,0]...Z[k,G-1]]^T$, $\mathbf{W}[k] = [W[k,0]...W_[k,G-1]]^T$, $H_1[k] = [H_1[k,0]...H_1,[k,G-1]]^T$, and $\mathbf{H}_2[k] = [H_2[k,0]...H_2[k,G-1]]^T$ are $G \times 1$ column vectors, each gth component representing

$$[\mathbf{Z}[k]]_g := Z[k,g] = \sum_{n=0}^{N-1} y[n,g]e^{-j\frac{2\pi kn}{N}}, \tag{31}$$

$$[\mathbf{W}[k]]_g := W[k,g] = \sum_{n=0}^{N-1} v[n,g]e^{-j\frac{2\pi kn}{N}}, \tag{32}$$

$$[\mathbf{H}_1[k]]_g := H_1[k,g] = \sum_{n=0}^{N-1} h_1[n,g]e^{-j\frac{2\pi kn}{N}}, \tag{33}$$

$$[\mathbf{H}_2[k]]_g := H_2[k,g] = \sum_{n=0}^{N-1} h_2[n,g]e^{-j\frac{2\pi kn}{N}}, \tag{34}$$

respectively. The replica signal is subtracted from the received signal through $p_{rx}(t)$ on each FS branch and the remaining User 2 signal is expressed as

$$\begin{aligned}\bar{\mathbf{Z}}_2[k] &= \mathbf{Z}[k] - \hat{\mathbf{Y}}_1[k] \\ &= \mathbf{H}_2[k]S_2[k] + \mathbf{W}[k] + \mathbf{R}_1[k],\end{aligned} \tag{35}$$

where $\bar{\mathbf{Z}}_2[k] = [\bar{Z}_2[k,g]...\bar{Z}_2[k,G-1]]^T$ is the signal after the first cancellation for demodulating the User 2 signal, and $\mathbf{R}_1[k] = [R_1[k,0]...R_1[k,G-1]]^T$ is the residual interference of the User 1 signal.

2.2 Second Cancellation

After the first cancellation, the User 2 signal is demodulated. As already stated, $v(t)$ is the filtered noise. When $v(t)$ is sampled at the Nyquist rate of $1/T_s$, the samples of $v(t)$ are independent one another. However, when the sampling rate is a multiple of the baud rate, the noise samples are correlated. Consequently, it is necessary to whiten the colored noise samples. In order to perform noise-whitening, it is required to calculate the noise covariance matrix on each subcarrier whose (g_1, g_2)th element is given as

$$\begin{aligned}&R_{W_{g1,g2}}[k] \\ &= E[W[k,g_1]W^*[k,g_2]] \\ &= \sigma_v^2 \frac{1}{N}\sum_{n_1=0}^{N-1}\sum_{n_2=0}^{N-1} p_{rx}((n_2-n_1+(g_2-g_1)/G)T_s) \\ &\quad \times \exp\left(j\frac{2\pi k(n_2-n_1)}{N}\right)\end{aligned} \tag{36}$$

where σ_v^2 is the noise variance. Multiplying both sides of Eq. (35) by $\mathbf{R}_W^{-\frac{1}{2}}[k]$,

$$\begin{aligned}&\mathbf{R}_W^{-\frac{1}{2}}[k]\bar{\mathbf{Z}}_2[k] = \mathbf{R}_W^{-\frac{1}{2}}[k](\mathbf{H}_2[k]S_2[k] + \mathbf{W}[k] + \mathbf{R}_1[k]), \\ &\tilde{\mathbf{Z}}_2[k] = \tilde{\mathbf{H}}_2[k]S_2[k] + \tilde{\mathbf{W}}[k] + \tilde{\mathbf{R}}_1[k].\end{aligned} \tag{37}$$

The output of the subcarrier-based maximum ratio combining (MRC) among the whitened samples is given as

$$\begin{aligned}\tilde{S}_2[k] &= \frac{\tilde{\mathbf{H}}_2^H[k]\bar{\mathbf{Z}}_2[k]}{\tilde{\mathbf{H}}_2^H[k]\tilde{\mathbf{H}}_2[k]} \\ &= \frac{(\mathbf{R}_W^{-\frac{1}{2}}[k]\hat{\mathbf{H}}_2[k])^{H_2}(\mathbf{R}_W^{-\frac{1}{2}}[k]\bar{\mathbf{Z}}[k])}{(\mathbf{R}_W^{-\frac{1}{2}}[k]\hat{\mathbf{H}}_2[k])^{\mathbf{H}_2}(\mathbf{R}_W^{-\frac{1}{2}}[k]\hat{\mathbf{H}}_2[k])}\end{aligned} \tag{38}$$

where $\hat{\mathbf{H}}_2[k] = [\hat{H}_2[k,0]...\hat{H}_2[k,G-1]]^T$ is the estimated frequency response on the kth subcarrier for the User 2 signal. The symbol of the User 2 signal, $\hat{S}_2[k]$, is detected based on $\tilde{S}_2[k]$. From $\hat{S_2}[k]$, the replica signal on each branch for cancelling the User 1 signal is generated in the $G \times 1$ vector form as

$$\hat{\mathbf{Y}}_2[k] = \mathbf{H}_2[k]\hat{S_2}[k]. \tag{39}$$

The replica signal is subtracted from the received signal as

$$\begin{aligned}\mathbf{Z}_1[k] &= \mathbf{Z}[k] - \hat{\mathbf{Y}}_2[k] \\ &= \mathbf{H}_1[k]S_1[k] + \mathbf{W}_1[k] + \mathbf{R}_2[k],\end{aligned} \tag{40}$$

where $\mathbf{Z}_1[k] = [Z_1[k,0]...Z_1[k,G-1]]^T$ is the signal after the second cancellation for demodulating the User 1 signal, and $\mathbf{R}_2[k] = [R_2[k,0]...R_2[k,G-1]]^T$ is the residual interference of the User 2 signal. Finally, the User 1 signal is demodulated with the same manner as Eqs. (38)–(40).

3. Numerical Results

3.1 Simulation Conditions

Simulation conditions are presented in Table 1. The symbols are modulated with QPSK or 64QAM for both of the User 1 and User 2 signals, and multiplexed with OFDM. The numbers of data subcarriers and pilot subcarriers are 48 and 4 while the DFT size is 64. The bandwidth of the subcarrier is 312.5 kHz. The oversampling rate, G, is 1 or 2, the

Table 1 Simulation conditions.

Modulation scheme	1st:QPSK, 64QAM 2nd:OFDM
Number of subcarriers	64
Number of data subcarriers	48
Bandwidth of subcarrier	312.5 [kHz]
Preamble length (GI+Preamble)	1.6 + 6.4[μs]
OFDM symbol length (GI+Data)	0.8 + 3.2[μs]
Number of OFDM symbols per packet	1
Number of OFDM packets per trial	100000
Oversampling rate	$G = 1, 2$
Channel model	Rayleigh (16 path)
Channel estimation	Ideal

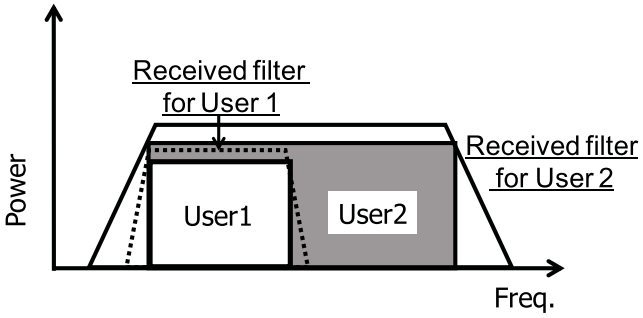

Fig. 5 Conventional channel allocation.

number of packets per trial is 100000, and the number of OFDM symbols per packet is 1. The channel responses of the subcarriers are estimated with the preamble symbols at the beginning of the packet. The orthogonal sequences for channel estimation are transmitted over multiple symbols in the time domain on each subcarrier. A different orthogonal sequence is transmitted for each user during the preamble symbols. The channel responses for the signals of User 1 and User 2 are estimated with the orthogonality between the sequences, respectively. For numerical evaluation through the simulation ideal channel estimation is assumed. As a channel model, 16 path Rayleigh fading with uniform delay profile is employed [9]. In the figures, "No interference" implies that only the User 1 signal occupies 2 channels and no interference exists. This means that the spectrum efficiency reduces to a half for the case of "G=2(No interference)". On the other hand, if the spectrum efficiency is maintained to the same as the proposed scheme and no imaging component is transmitted, the BER performance is equal to that of "G=1(No interference)". In this case, no diversity is realized. For the conventional scheme in [7], the channel allocation in Fig. 5 is employed. User 2 transmits the imaging components that are overlapped with the signal for User 1. As the same transmission distance is assumed the signal powers of the users are unified. This condition is different from [7] since the assumption of the distances is different.

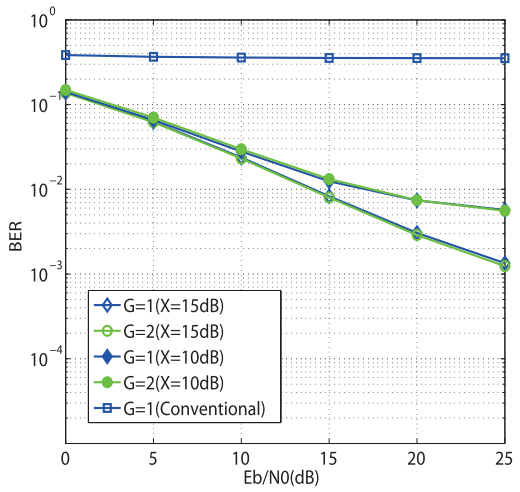

Fig. 6 BER vs. E_b/N_0 of the first demodulation (QPSK).

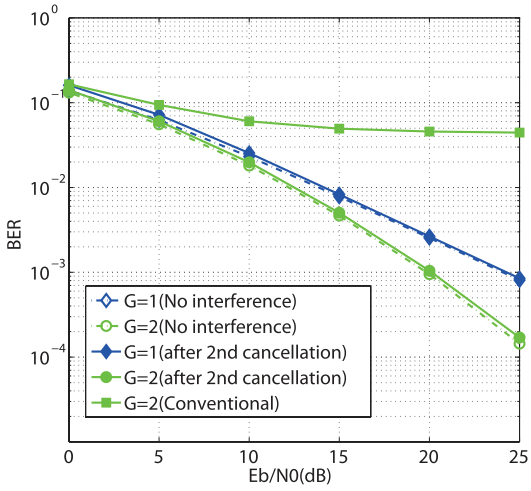

Fig. 7 BER vs. E_b/N_0 after the second cancellation (QPSK, X=15 dB).

3.2 BER Performance with QPSK Modulation

Figure 6 shows the relationship between the BER and E_b/N_0 for the first demodulation before cancellation. In the proposed scheme, the power difference between the desire and imaging components is set to X=15 dB or X=10 dB. In the conventional scheme, as Fig. 5 shows, the imaging component of User 2 is overlapped to the desired signal of User 1 with the same signal power. Therefore, the first demodulation before the cancellation causes many symbol errors in the conventional scheme. On the other hand, the BER performance of proposed scheme with X=15 dB is smaller than that with X=10 dB. This is because the amount of imaging component causes the interference to the desired signal.

Figure 7 shows the relationship between the BER and E_b/N_0 for X=15 dB after the second cancellation. The OFDM scheme without the imaging component ("G=1(No interference)") follows the BER curve on a Rayleigh Fading channel without diversity. On the other hand, "G=2(No

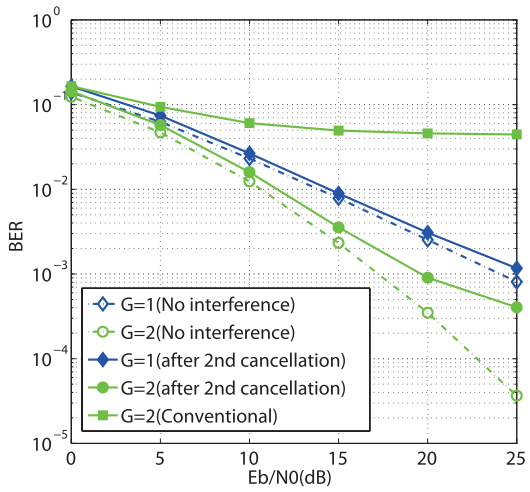

Fig. 8 BER vs. E_b/N_0 after the second cancellation (QPSK, X=10 dB).

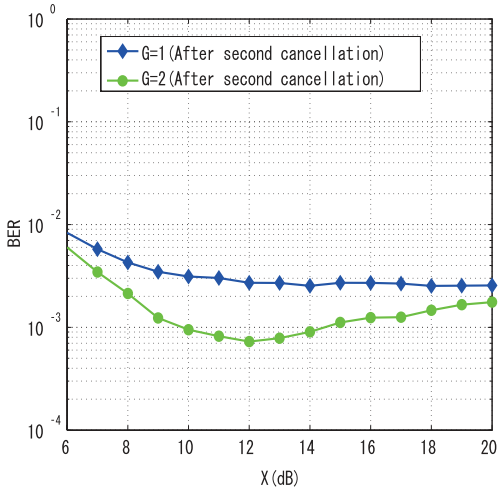

Fig. 9 BER vs. X after second cancellation (QPSK, E_b/N_0=20 dB).

interference)" shows the BER curve with diversity gain because of FS. In the conventional scheme, the first demodulation for the signal of User 1 before the cancellation causes more symbol errors and the large residual interference. As a result, due to this residual interference, the BER performance of the User 2 signal does not improve even with FS. As for the proposed scheme, if the power difference is 15 dB, the replica of the User 2 signal is regenerated accurately and the interference to the User 1 signal is eliminated with the proposed scheme. Path diversity with FS is then realized. Therefore, the proposed scheme shows better BER curves than those with no FS diversity (G=1).

Figure 8 shows the relationship between the BER and E_b/N_0 for X=10 dB after the second cancellation. In this case, the signal to interference plus noise ratio (SINR) is lower before the first cancellation than that with X=15 dB. Lower SINR leads to higher error rates on the tentative detection of the User 1 signal even though more diversity gain can be expected with larger imaging components. The interference due to the detection errors then increases and the BER curve of the proposed scheme with FS (G=2) exhibits an error floor. On the other hand, the same as that in Fig. 7, the BER of the conventional scheme does not improve with FS.

Figure 9 shows the relationship between the BER and the power difference X after the second cancellation. E_b/N_0 is set to 20 dB. When X is close to 12 dB, the BER is the smallest. If X is larger than 12 dB, the BER increases because the SINR is low before the first cancellation and the more tentative detection errors occur. If X is smaller than 12 dB, the BER also grows. In this case the proposed scheme can not obtain diversity gain since the power of the imaging components for FS diversity is smaller.

Figure 10 shows the relationship between the BER and the number of cancellation processes. E_b/N_0 is 20 dB and X is set to 10 dB. Due to the residual interference, the BER does not improve even though the number of cancellation processes increases from 1 to 4. Thus, the accuracy of the first demodulation mainly determines the BER in this scheme.

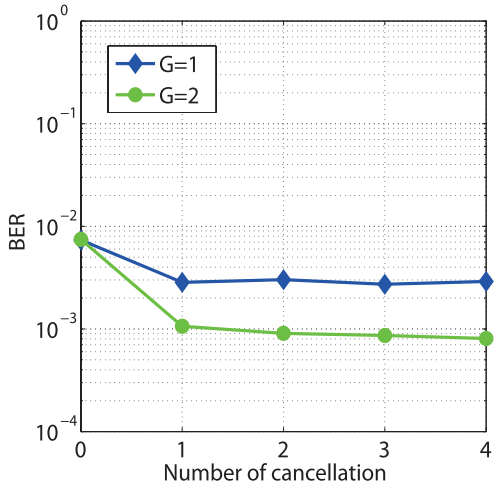

Fig. 10 BER vs. Number of cancellation processes (QPSK, E_b/N_0 = 20 dB, X = 10 dB).

3.3 BER Performance with 64QAM

Figures 11 and 12 show the BER performance versus E_b/N_0 after the second cancellation. In the conventional scheme, the same as QPSK modulation, the first demodulation before the cancellation causes more symbol errors and the large residual interference. As a result, the same as those in Figs. 7 and 8, due to this residual interference, the BER performance does not improve by FS. As for the proposed scheme, different from the BER curves with QPSK modulation, only a small amount of diversity gain can be obtained with FS even though the power of the imaging component changes. This is because 64QAM modulation is less robust to the interference. Therefore, the first demodulation before the first cancellation causes more symbol errors and the residual interference limits path diversity gain.

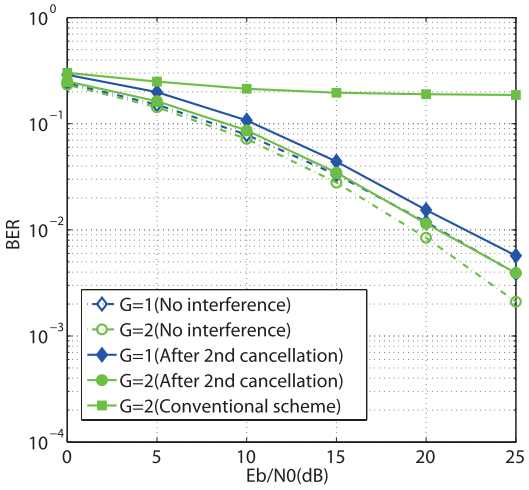

Fig. 11 BER vs. E_b/N_0 after the second cancellation (64QAM, X=15 dB).

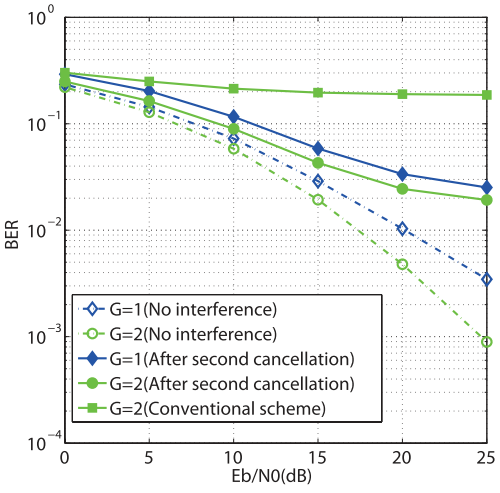

Fig. 12 BER vs. E_b/N_0 after the second cancellation (64QAM, X=10 dB).

The BER performance versus the number of cancellation for 64QAM modulation is shown in Fig. 13. E_b/N_0 is 20 dB and X is set to 10 dB. The same as the above explanation, due to the residual interference, the BER improves only a little even though the number of cancellation processes increases from 1 to 4. Thus, the accuracy of the first demodulation mainly determines the BER in this scheme.

4. Conclusions

In this paper, non-orthogonal access over multiple channels with IIC and FS is proposed. In the proposed scheme, the replica signal is regenerated and subtracted from the received signal for each desired signal. The proposed scheme improves the BER performance when the power difference between the desire and imaging components is large enough in order to suppress the interference by the diversity gain with FS. Numerical results through computer simulation

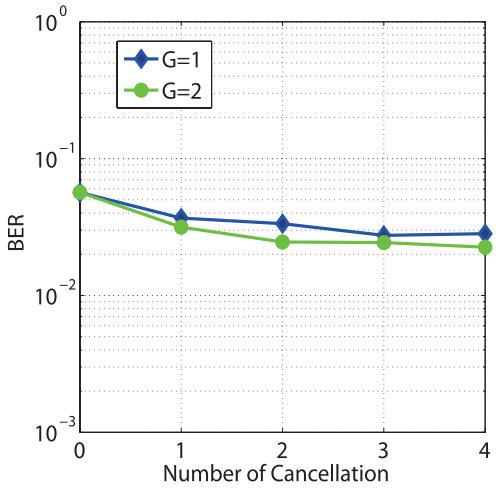

Fig. 13 BER vs. Number of cancellation processes (64QAM, E_b/N_0 = 20 dB, X = 10 dB).

have shown that non-orthogonal access on multiple channels is realized. The proposed scheme can obtain diversity gains for non-orthogonal signals modulated with QPSK and transmitted with the same power. On the other hand, the proposed scheme with 64QAM can not realize diversity since 64QAM modulation is not robust to the interference and the errors on the first demodulation increases the interference through the cancellation process.

In the proposed system, the accuracy of the first demodulation has a large significance on the BER performance. Therefore, as future works, the performance of the system with a more efficient demodulation algorithm such as MLD or MMSE will be investigated.

Acknowledgement

This work is supported in part by a Grant-in-Aid for the Global Center of Excellence for high-Level Global Cooperation for Leading-Edge Platform on Access Spaces.

References

[1] R. Nee, G Awater, M. Morikura, H. Takanashi, M. Webster, and K. Halford, "New high-rate wireless LAN standards," IEEE Commun. Mag., vol.37, no.12, pp.82–88, Dec. 1999.
[2] S. Weinstein, "The history of orthogonal frequency division multiplexing," IEEE Commun. Mag., vol.47, no.11, pp.26–35, Nov. 2009.
[3] A.N. Barreto, "Antenna transmit diversity for wireless OFDM systems," IEEE 55th Vehicular Technology Conference, vol.2, pp.757–761, May 2002.
[4] J. Salz and J.H. Winters, "Effect of fading correlation on adaptive arrays in digital mobile radio," IEEE Trans. Veh. Technol., vol.43, no.4, pp.1049–1057, Nov. 1994.
[5] R.C. Kizilirmak and Y. Sanada, "Multipath diversity through time shifted sampling for spatially correlated OFDM-antenna array systems," IEICE Trans. Fundamentals, vol.E91-A, no.11, pp.3104–3111, Nov. 2008.
[6] C. Tepedelenlioğlu and R. Challagulla, "Low-complexity multipath diversity through fractional sampling in OFDM," IEEE Trans. Signal Process., vol.52, no.11, pp.3104–3116, Nov. 2004.

[7] H. Osada, H. Nishimura, M. Inamori, and Y. Sanada, "Adjacent channel interference cancellation in fractional sampling OFDM receiver," IEEE 74th Vehicular Technology Conference, Sept. 2011.
[8] T. Shinkai, H. Nishimura, and Y. Sanada, "Improvement on diversity gain with filter bandwidth enlargement in fractional sampling OFDM receiver," IEICE Trans. Commun., vol.E93-B, no.6, pp.1526–1533, June 2010.
[9] Joint Technical Committee of Committee T1 R1P1.4 and TIA TR46.3.3/TR45.4.4 on Wireless Access, "Draft final report on RF channel characterization," Paper no.JTC(AIR)/94.01.17-238R4, Jan. 1994.

Hiroyuki Osada was born in Yamanashi, Japan in 1986. He received his B.E. degree in electronics engineering from Keio University, Japan in 2011. Since April 2011, he has been a graduate student in School of Integrated Design Engineering, Graduate School of Science and Technology, Keio University. His research interests are mainly concentrated on software defined radio.

Mamiko Inamori was born in Kagoshima, Japan in 1982. She received her B.E. and M.E. degrees in electronics engineering from Keio University, Japan in 2005 and 2007 respectively. Since April 2007, she has been a Ph.D. candidate in School of Integrated Design Engineering, Graduate School of Science and Technology, Keio University. Her research interests are mainly concentrated on software defined radio.

Yukitoshi Sanada was born in Tokyo in 1969. He received his B.E. degree in electrical engineering from Keio University, Yokohama Japan, his M.A.Sc. degree in electrical engineering from the University of Victoria, B.C., Canada, and his Ph.D. degree in electrical engineering from Keio University, Yokohama Japan, in 1992, 1995, and 1997, respectively. In 1997 he joined the Faculty of Engineering, Tokyo Institute of Technology as a Research Associate. In 2000 he jointed Advanced Telecommunication Laboratory, Sony Computer Science Laboratories, Inc, as an associate researcher. In 2001 he jointed Faculty of Science and Engineering, Keio University, where he is now a professor. He received the Young Engineer Award from IEICE Japan in 1997. His current research interest is in software defined radio, cognitive radio, and OFDM.